NASA TECHNICAL MEMORANDUM

NASA TM X-68289

NASA TM X-68289

NOISE COMPARISONS FROM FULL-SCALE FAN TESTS AT NASA LEWIS RESEARCH CENTER

by Marcus F. Heidmann and Charles E. Feiler
Lewis Research Center
Cleveland, Ohio

TECHNICAL PAPER proposed for presentation at
Aero-Acoustics Conference sponsored by the
American Institute of Aeronautics and Astronautics
Seattle, Washington, October 15 - 17, 1973

NOISE COMPARISONS FROM FULL-SCALE FAN TESTS AT NASA LEWIS RESEARCH CENTER

Marcus F. Heidmann* and Charles E. Feiler+
National Aeronautics and Space Administration
Lewis Research Center
Cleveland, Ohio

Abstract

The overall aero and acoustic design features of eight 6-foot-diameter, single-stage fans tested in an outdoor acoustic facility are described. A correlation of the acoustic results for subsonic tip-speed fans showed the total sound power to be proportional to the mechanical power imparted to the fan and the specific work performed on the air to within ±2 dB. The correlation was relatively insensitive to fan design variables over a broad range of operating conditions. Maximum perceived noise levels were generally proportional to the sound power levels with both noise levels exhibiting a relatively unique increase with fan pressure ratio when normalized by the delivered thrust.

The spectra of broadband noise attributed to the fan exhibited a bimodal characteristic for most of the fans. A predominant mode centered near the blade-passage tone and another at 8 to 16 times the tone frequency. The broadband power level also varied with mechanical power and specific work, but at a level about 3 dB below the total power. The power level of the blade-passage tones was related to the relative Mach number at the rotor tip.

Introduction

The NASA Lewis Research Center has been engaged for the past four years in a broad-ranging program of research in fan noise generation and suppression. This research was started in support of the Quiet Engine Program for CTOL application and more recently has been in support of quiet propulsion for STOL application.

Acoustic testing at NASA-Lewis is primarily accomplished on an outdoor facility with fans of six-foot diameter. With this facility, far-field acoustic data are obtained in both the inlet and exit quadrants of the full-scale fans. In addition, in-duct acoustic data and aerodynamic performance data are obtained.

To date, eight 6-foot-diameter, single-stage fans have been evaluated covering a broad range of fan design pressure ratios (1.2 to 1.6) and fan tip speeds (700 to 1550 ft/sec). Each fan is generally tested along three operating lines (nozzle areas) over a speed range from 60 percent to 90 percent of the design speed corresponding to engine approach and takeoff speeds, respectively. Some of the stages have also been evaluated with acoustically-treated inlet and exhaust ducts, but this paper will be restricted to results from unsuppressed configurations. The eight fans embodied a variety of acoustic principles, insofar as aerodynamics permited, to obtain low noise. The aero design and acoustic results for some of these fans have been previously discussed.(1-4)

This paper will describe the full-scale fans that have been tested and some correlations of total acoustic power and perceived noise levels based on fan overall design and performance parameters. In addition, the acoustic power spectra for each fan are examined for distinctive properties of broadband and blade-passage-tone noise. Characteristic properties and correlations of these noise components are presented.

Full-Scale Fan Test Facility

The fan test facility is shown in the photograph of Figure 1. The fan test package to the left is driven by a shaft leading to the main drive motor of the Lewis 10x10-foot supersonic wind tunnel housed in the building to the right. The centerline of the facility is 19 feet above the asphalt surface of the site. Figure 2 shows a cutaway sketch of the fan test package. The fan is supported by an internal pylon housing the bearings and associated gear. The fans are generally driven through the inlet, but some experiments have been performed with a rear drive to evaluate possible facility related airflow distortion effects caused by shaft and fan support structures.

A plot plan of the test site is shown in Figure 3. Far-field microphones are located at 10° intervals on a 100-foot arc. The fan package is some 120 feet from the wall of the drive building. This wall is covered with six inches of polyurethane foam to reduce sound reflections. There are no other nearby obstacles to reflect sound.

Signals from the microphones are recorded on tape and subsequently reduced with appropriate averaging times to 1/3-octave sound pressure levels. The 1/3-octave frequency bands from 50 to 20,000 Hz are covered. Three separate data samples are averaged at each test condition to yield the final data. The data are corrected from test day temperature and humidity to a standard temperature of 59° F and to a relative humidity of 70 percent. Acoustic data are taken separately from runs in which aerodynamic data are taken. No data are taken during any kind of precipitation or at wind velocities above five knots.

Fan Stage Aero-Acoustic Design

The acoustic features and aerodynamic parameters of the fan stages will be discussed in this section. Several noise reduction principles were used in the design of each fan stage: (1) All stages were designed without inlet guide vanes; (2) a rotor-stator axial spacing of at least two true rotor chords was used; and (3) rotor and stator blade numbers were selected so that the blade-passage-frequency tones due to rotor-stator interaction would be cutoff. Two of the fans were de-

*Aerospace Research Engineer, Member AIAA
+Head, Acoustics Section, Member AIAA

signed according to the theory of Kemp, Sears, and Horlock[5,6] that relates rotor-stator interaction noise to lift fluctuations on the stator. According to this theoretical treatment, it is beneficial to increase the chord of the downstream blade row, in this case the stator. When this was done, stator blade number was reduced to avoid stator solidities that were unacceptably large, and the cutoff criteria could not be met for these two stages.

At the outset of the program, the acoustic tradeoff between aerodynamic loading and fan tip speed, if any, was not known. Accepted fan noise generation correlations indicated a fifth power dependence of noise on fan tip speed. This motivated a desire to keep tip speeds low at the considerable penalty of an increased number of drive turbine stages that an engine would require. Because of the limited experience relating to this possible tradeoff, the matrix of fans to be tested was selected to provide an evaluation of fan loading relative to fan tip speed. Figure 4 shows the matrix of fans. In this figure, fan pressure rise is plotted against fan tip speed.

To complete the characteristics of the overall fan designs, a third parameter, the work coefficient, $(\Delta\overline{V_\theta}/U_T)$, is included in addition to fan pressure rise and tip speed. This parameter is used herein as the indicator of the overall loading of the fan. In Figure 4, several lines of constant $(\Delta\overline{V_\theta}/U_T)$ are shown. It can be seen that several of the fans have about the same value of the work coefficient implying similar overall aerodynamic characteristics. It can also be seen that a range of the work coefficient parameters is covered at both constant pressure ratio and at constant tip speed. It should be noted that these fans were designed for a normal range of limiting values of the local blade diffusion factor or aerodynamic loading.

A more complete tabulation of the fan design parameters is given in Table I. The hub-tip ratio and specific flow were about 0.5 and 41 lbs/sec/ft^2, respectively, for all fans. It can be seen that the designs encompass a broad range of each parameter. The last fan listed, QF-9, has variable-pitch rotor blades to provide thrust reversal capability. This fan has a very low number of blades to facilitate the variable pitch and to keep the blade-passage frequency tone well below the frequency range of maximum annoyance. Figure 5 is a photograph of this fan while Figure 6 is a photograph of high-speed fan C.

Correlations of Overall Acoustic Performance

The data obtained for each fan stage consisted of 1/3-octave sound pressure spectra at 10° intervals from 10° to 160° measured on a 100-foot arc from the fan inlet. Fan speeds in 5 to 10 percent increments from about 60 to 90 percent of the design speed were run generally for three nozzle areas. These tests yielded a considerable amount of noise data.

For a preliminary study of the data, it was convenient to examine the behavior of two measures of noise as functions of overall fan design or operating conditions. These are: (1) the total sound power measured in dB relative to 10^{-13} watts, obtained by integration over all frequencies and angular positions; and (2) the maximum sideline value of perceived noise level. The first quantity provides a measure of the total sound produced without regard to frequency or directivity while the second quantity emphasizes the sound at those frequencies found to be most annoying to people. These noise parameters were examined with respect to overall fan design and performance parameters to determine overall correlations of the data.

Sound Power Correlation

The correlation that has been developed starts with the assumption given by the expression

$$\text{Sound Power} = \eta_c \times \text{shaft power} \qquad (1)$$

where η_c is the conversion efficiency to be evaluated functionally from the data. The size or scale of the fan as it influences noise is already established by the use of shaft power in Equation (1). The conversion efficiency η_c was found to vary linearly with the specific work performed by the fan and given by the total temperature rise, ΔT, across the stage. This is shown in Figure 7 where both η_c and PWL $-10 \log_{10}$ shp (a proportionally equivalent quantity in acoustic notation) are plotted against ΔT for tests made along the nominal operating line of each fan. The relationships determined from Figure 7 are

$$\eta_c = 0.955 \times 10^{-6}\ \Delta T \qquad (2)$$

and

$$\text{PWL} = 98.5 + 10 \log \Delta T + 10 \log \text{shp} \qquad (3)$$

where PWL is in dB (re 10^{-13} watts), ΔT is in °R, and shp is in horsepower. Figure 8 shows the data for all operating conditions tested and plotted according to Equation (3). Except for the high-speed fan C, the total scatterband shown is ± 2 dB. Fan C does not fall into the general class of fans represented by the bulk of the data as is shown by its larger sound output. This is due to the significant presence of multiple-pure tones. However, it should be noted that fan C approaches the correlation band at low speeds where multiple-pure tones are less severe. The correlations of Figure 8 show the sound power to depend linearly on the product of total power (shp) and specific work given by ΔT.

Alternate Forms of Correlation

Equation (3) can be expressed in several equivalent forms using other fan parameters. Beranek[7] gives as a correlation for ventilating fans the relation

$$\text{PWL} = 138 + 20 \log \text{shp} - 10 \log q \qquad (4)$$

where q is in cubic feet per minute, and shp is the rated motor horsepower of the fan drive unit. This relation converted to the form of Equation (3) is

$$\text{PWL} = 104.5 + 10 \log \Delta T + 10 \log \text{shp} \qquad (5)$$

It can be seen that Equation (5) yields sound power levels 6 dB larger than Equation (3) yields. However, it should be noted that the difference is less than 6 dB because rated motor horsepower is always larger than the delivered power used in the correlation given by Equation (3). Exact agreement would occur with a conservative assumption of a rated power equal to twice the delivered power.

Lowson[8] has obtained an expression starting from a mechanistic approach to the noise generation process that shows a linear dependence on fan area and a fifth power dependence on fan design tip speed. Equation (3) can also be expressed in this functional form by the use of approximate parametric relations for fan stages and is given by

$$PWL = K + 10 \log A + 50 \log U_T \qquad (6)$$

where A is the fan flow area, U_T is the tip speed, and K is a constant that depends on the particular fan design parameters.

Finally, Equation (3) can be converted to show the dependence of sound power on the more commonly used design parameters of thrust, F, and fan pressure ratio, Pr. In this form, Equation (3) becomes

$$PWL = 121.9 + 14 \log (Pr - 1) + 10 \log F \qquad (7)$$

For this relation, a fan efficiency of 0.85 was assumed. Figure 9 shows these data plotted in the form of Equation (7). It can be seen that the total scatterband is of the order of ±2.5 dB.

Perceived Noise Correlation

Figure 10 shows the maximum perceived noise levels on a 1000-foot sideline plotted in the functional form of Figure 9. The line through the data is in the exact functional form appearing in Equation (7) with the constant term adjusted to fit the data. The resulting relation is given by

$$PNL = 62.4 + 14 \log (Pr - 1) + 10 \log F \qquad (8)$$

The scatterband of the data is ±2.5 dB, the same as found in the sound power correlation. The similarity between the correlations of sound power and perceived noise is surprising considering that the blade-passage tone among all the data varied by an order of magnitude.

Although the correlation appears reasonably good, it can be seen that the trend of the data follows a dependence on fan pressure rise slightly greater than the line shows. This trend could be accounted for by the shift of the spectra to frequencies of higher annoyance as fan pressure rise (tip speed) increases for each fan. This effect can probably be accounted for at the expense of complicating the simple correlation; however, the correlation still provides a means of predicting fan perceived noise within 2.5 dB over a wide range of design and performance parameters.

Within the data spread around the correlations given by Equations (7) and (8) for the subsonic tip speed fans, there were no obvious trends that could be related to other fan design variables, such as loading or tip speed. The fans appear to behave as a class reasonably well represented by the correlations shown. When the tip speed exceeded sonic, as with fan C, the occurrence of multiple-pure-tone noise provided a significant noise increment above the level found at subsonic tip speeds. Since the multiple-pure tones are related to shock waves on the blade-leading edges, the correlation of this noise will depend on the relative inlet Mach number of the rotor.

Noise Spectra Analysis

Both broadband and tone noise contribute to the total acoustic power and perceived noise levels used in the previous correlations. A next step in the analysis is to examine the acoustic power spectra for broadband and tone content and to compare the behavior of the acoustic power of these noise components with the behavior found for the total acoustic power. The specific spectral composition of each fan is also important because it can show similarities and differences in these fans which are not reflected in total power measurements. In this preliminary study of the spectral data, attention will be focused on the broadband noise underlying the blade-passage tones while exhaust jet and multiple pure tone noise behavior will be neglected at this time.

Properties of the Acoustic Spectra

An examination of spectral data from these fans (1/3-octave power spectra, as well as narrow band and 1/3-octave sound pressure spectra at various angular positions) revealed some characteristic similarities and differences in the spectral shapes for the various fans tested. These similarities were especially pronounced with respect to the apparent broadband noise level generated by the fan stage. Similarities in the apparent broadband spectra were observed both for a given fan as speed was varied, and from fan to fan at the same speed. These similarities in the broadband spectra were observed from suitable superposition of the sound power spectra.

The broadband noise underlying the tones is often uncertain from an inspection of 1/3-octave intervals. This overlapping or straddling of 1/3-octave intervals by the tones varies with a change in fan operating speed. In an attempt to minimize the uncertainties in broadband spectra caused by the straddling, a superposition of 1/3-octave power spectra for four speed conditions for each fan was used. The superposition was accomplished by a systematic translation of the spectra. The frequency abscissa was first aligned by a translation proportional to the change in fan speed. The power level ordinate was then adjusted to superimpose the spectra in a high-frequency region where narrow-band analysis implied a relative freedom from blade-passage tones. For comparison from fan to fan at a given speed, the frequency shift was made with respect to blade-passing frequency.

Figure 11(a) illustrates the results of superimposing sound power spectra for different speeds for a given fan. The superimposed spectra show that the fan has a high degree of self-similarity in the fan broadband area with changes in speed. This self-similarity with speed was observed for all of the fans.

Figure 11(b) shows a superimposed plot for fans QF-3 and QF-9 at the same speed. Again, a similarity of the spectra is observed in the region of the blade-passage tones and their harmonics. However, the QF-3 fan exhibits a relatively "rapid" and uniform "fall-off" of the high frequency portion of the spectra compared to the QF-9 fan where the "fall-off" is relatively "slow" and irregular. This difference in spectral shape (noted to a lesser degree in the other fans) was taken to imply a

difference in broadband noise generation in these two fans.

Analytical Representation

The broadband noise spectral shape for a fan is inferred by the baseline underlying the tones in the 1/3-octave displays. In many instances, the establishment of this baseline, or apparent broadband variation, is a matter of judgment based on inspection of both the 1/3-octave and narrow-band spectra.

A method of characterizing the superimposed apparent broadband noise profiles for these fans (Fig. 11(a)) which provides for the difference in spectral shapes observed in Figure 11(b) is illustrated in Figure 12. The estimated apparent broadband profile is shown by the solid line. It was found that, in all cases, the estimated apparent broadband profile could be characterized by a bimodal log normal distribution shown by the dashed line in Figure 12. The center frequency of the primary (low frequency) mode is given by f_p, and the center frequency of the secondary (high frequency) mode is given by f_s. A log normal distribution function with a geometric deviation, σ, of 2.2 was used for this purpose. Inspection of the octave and narrow-band spectra showed that this distribution function was adequate for the resolution of spectral content desired in this preliminary analysis of the data. The equation for the power level distribution with frequency for a log normal distribution is given by

$$PWL = PWL_{max} + 10 \log_{10} e^{-\frac{1}{2}\left(\frac{\ln f/f_p}{\ln \sigma}\right)^2} \qquad (9)$$

Figures 13(a) through (h) show the combination of primary and secondary (low and high frequency) modes fitted to each set of superimposed fan spectra. For consistency, two modes are shown for each fan even though the high-frequency mode may be negligible or obscure. The high-frequency mode is shown by a dashed curve when highly uncertain to imply a maximum probable level. The general "fit" of the bimodal for normal distribution to the apparent broadband noise variation is seen to be quite good for all of the fans.

Discussion of Broadband Characterization

The broadband noise characterizations used in Figure 13 show some distinctive properties of the fans. The lower frequency mode of broadband noise dominates the broadband spectra for most fans. It appears typical of what has been observed in other fan tests and is often attributed to turbulent condistions entering the fan.

The high frequency mode of broadband noise is obscure in some fans and difficult to resolve in all fans because of a lack of higher frequency data. The high-frequency mode is strongly evident in fans B and QF-9 where low blade-passage frequency appears to make it more evident. Additional analysis has shown that this high-frequency mode is more pronounced in the forward quadrant spectra which implies that it originates from the fan inlet. Distinctive spectral properties of broadband noise at high frequencies have been discussed and analyzed by various investigators.(9,10,11) Vortex shedding from both leading and trailing edges of airfoils have been proposed as possible sources. Identification and control of such sources within a fan spectrum, however, remain uncertain.

Some additional evidence on the generation of broadband noise in a high-frequency mode was provided by exploratory tests with fan QF-9 directed toward reducing inlet flow distortions. Tests were made using a fine mesh screen in front of the fan inlet. The power spectra obtained from such tests is shown in Figure 14. A high-frequency mode of broadband noise was generated with a center frequency of the order of the Strouhal frequency for flow over the screen wire size. The flow over the screen will generate broadband noise of this type, but the power level observed (equivalent to the blade-passage tones) is higher than expected. The result suggests that turbulent flow properties entering or generated within the fan stage can be the cause of a high level, high frequency broadband noise with definite spectral properties emanating from the fan.

The primary, or low-frequency, broadband mode is seen in Figure 13 to center and peak near the second and third harmonic of the blade-passage frequency in all cases. Analysis of the secondary or high-frequency mode is highly qualified because of the difficulty in identifying the presence and exact location of this mode. From a general observation of Figure 13, the center frequency does not appear to vary directly with the change in speed. For example, both the fan B and QF-9 spectra suggest that a better superposition at high frequencies is possible with a different frequency translation than that used in Figure 13. The available data, however, preclude a more refined study at this time.

Plots of the variation of center frequency for the two broadband modes contained in the bimodal distributions as shown in Figure 13 are given in Figure 15. The center frequency of the low-frequency mode is about 2-1/2 times the blade-passage frequency, while the center of the high-frequency mode is about 8 to 16 times the blade-passage frequency. On the average, it appears that the center frequency of the secondary mode is about four times that of the primary mode, but the data do not give convincing evidence of such a relationship.

Fundamentally the center frequency of broadband noise obtained from a power spectral density analysis has more significance with regard to its origin. Interestingly, a log normal distribution retains its log normal properties when transformed to a power spectral density display. Preliminary analysis of the spectral density indicated that the mode centers between the first and second harmonic of the blade-passage frequency which is near the mean power frequency from blade-passage tones. The close relationship between this low-frequency broadband noise and blade-passage tones implies a common source, but this may be a coincidence resulting from some similarity of aero design for all of these fans.

Correlation of Component Noise

The analytical representation of the apparent broadband power spectra by a bimodal log normal distribution facilities numerical calculations for the sound power contained in this broadband component. The power content of the blade-passage tones can then be obtained by subtraction of the broadband

power from the total power in the region of applicability.

Fan Broadband Noise

The total broadband power (the sum of the powers in the low- and high-frequency modes of the normal distributions) is plotted in Figure 16 and compared to the mean level of the total sound power as obtained from Figure 7. The mean value of the total broadband power is about 3 to 3.5 dB less than the total power, indicating the same dependence of broadband noise on overall total temperature rise (specific work) and shaft horsepower. The mean value of the total broadband power is given by

$$(PWL)_{BB} = 95.3 + 10 \log \Delta T + 10 \log shp \quad (10)$$

The sound power contained in the low-frequency mode of broadband noise (from an integration of the primary log normal distribution) is shown in a correlation comparable to that used for total broadband power in Figure 17. This broadband noise has a functional variation similar to total broadband sound power, but the level is about 1 dB lower. Of some significance, the supersonic tip speed fan, fan C, gives a primary broadband noise level comparable to the lower tip speed fans.

The sound power contained in the secondary or high-frequency mode is shown in Figure 18. It is apparent from the large spread in data that other fan parameters beside the shaft power and work input affect the power contained in this mode. Obviously, reliable correlation and characterization of this mode must await a more precise analysis.

Blade-Passage-Tone Noise

The power contained in the blade-passage tone and its harmonics was obtained from the difference between total power and broadband power over the appropriate frequency region. Figure 19 shows that the power in the tones does not correlate with shaft power and work input as might be expected because of such correlations for broadband power and total power. Figure 19, however, does illustrate the magnitude of the tone power with regard to the broadband power. The tone power is not consistently higher or lower than broadband power and its level seems to vary with both operating condition and fan design. Apparently the broadband and total power exhibit similar correlations because of a combination of broadband dominance and unusual tone behavior.

Tone generation is often related to rotor tip speed. One correlation which appears to describe the tone behavior is shown in Figure 20. Tone power normalized by the total mass flow rate is shown to vary with the 5th power of the rotor tip relative inlet Mach number. A significant deviation from this trend occurs near a Mach number of unity. The tone power decreases above a Mach number near one. This decrease may be attributed to the propagation of tone power as multiple-pure tones which remain to be analyzed.

For a given fan, where mass flow rate is proportional to tip speed, the correlation in Figure 20 gives a sixth power dependence of tone power with tip speed. Broadband power varies with shaft power and work input which for a given fan gives a fifth power dependence with tip speed. This difference in tip speed dependency can cause the total source power of a given fan to shift from broadband dominance to tone dominance with increasing tip speed.

Concluding Remarks

These studies of full-scale fan noise have shown that for a range of state-of-the-art fan designs, useful correlations of overall noise given by sound power level and perceived noise level can be obtained with overall fan performance parameters such as the shaft power and specific work, or fan thrust and fan pressure ratio. The correlations are useful for both sound power and perceived noise predictions to within ± 2.5 dB, and are limited to fans with no strong multiple-pure-tone generation.

A closer examination of the fan power spectra in terms of broadband and blade-passage-tone noise has provided additional noise comparisons. The total fan broadband noise power has a functional dependance on fan parameters similar to that for total power but at a level 3 to 3.5 dB lower. The fan broadband noise appears to originate from two sources which give spectral modes that appear to have log normal distributions which are separated in center frequencies. The lower frequency mode usually dominates the fan broadband noise and is centered near the blade-passage frequency. A higher frequency mode was pronounced in a few fans. Its functional dependence differed from the low-frequency mode, but could not be determined from the limited amount of data.

The sound power in the blade-passage tones appears to vary with the relative inlet Mach number at the rotor tip rather than shaft power and specific work. This difference can cause total power to be either broadband or tone dominated depending on the specific design and operating condition.

The preliminary spectral analysis of the sound power has provided some initial insight into similarities and differences of the fans tested. A continuing analysis should prove useful for both better predictions of noise levels and a better understanding of noise mechanisms.

References

1. Anon., "Aircraft Engine Noise Reduction," SP-311, 1972, NASA, Washington, D. C.

2. Leonard, B. R., Schmiedlin, R. F., Stakolich, E. G., and Neumann, H. E., "Acoustic and Aerodynamic Performance of a 6-Foot-Diameter Fan for Turbofan Engines. I - Design of Facility and QF-1 Fan," TN D-5877, 1970, NASA, Cleveland, Ohio.

3. Goldstein, A. W., Lucas, J. G., and Balombin, J. R., "Acoustic and Aerodynamic Performance of a 6-Foot-Diameter Fan for Turbofan Engines. II - Performance of QF-1 Fan in Nacelle Without Acoustic Suppression," TN D-6080, 1970, NASA, Cleveland, Ohio.

4. Montegani, F. J., "Noise Generated by Quiet Engine Fans. I - Fan B," TM X-2528, 1972, NASA, Cleveland, Ohio.

5. Kemp, N. H., and Sears, W. R., "The Unsteady Forces Due to Viscous Wakes in Turbomachines," Journal of the Aeronautical Sciences, Vol. 22, No. 7, July 1955, pp. 478-483.

6. Horlock, J. H., "Fluctuating Lift Forces on Aerofoils Moving Through Transverse and Chordwise Gusts," Journal of Basic Engineering, Vol. 90, No. 4, Dec. 1968, pp. 494-500.

7. Beranek, L. L., ed., Noise Reduction, McGraw-Hill, New York, 1960.

8. Lowson, M. V., "Theoretical Studies of Compressor Noise," CR-1287, 1969, NASA, Washington, D. C.

9. Metzger, F. B., and Hanson, D. B., "Low-Pressure-Ratio Fan Noise Experiment and Theory," Paper 72-GT-40, Mar. 1972, ASME, New York, N. Y.

10. Barry, F. W., and Magliozzi, B., "Noise Detectability Prediction Method for Low Tip Speed Propellers," HSER-5834, AFAPL-TR-71-37, AD-729432, June 1971, Hamilton Standard, Windsor Locks, Conn.

11. Goldstein, A. W., Glaser, F. W., and Coats, J. W., "Effect of Casing Boundary-Layer Removal on Noise of a Turbofan Rotor," TN D-6763, 1972, NASA, Cleveland, Ohio.

TABLE I. - FAN DESIGN PARAMETERS

FAN	PRESSURE RATIO	TIP SPEED, FT/SEC	BLADE NO.	VANE NO.	CUTOFF	BPF, Hz	ROTOR SOLIDITY	DESIGN BY
QF-1	1.5	1107	53	112	YES	3120	1.34	LEWIS
A	1.5	1160	40	90	YES	2420	1.45	G.E.
B	1.5	1160	26	60	YES	1570	1.30	G.E.
QF-3	1.4	1107	53	112	YES	3120	1.34	LEWIS
QF-5	1.6	1090	36	88	YES	2180	1.38	P&WA
C	1.6	1550	26	60	YES	2250	1.40	G.E.
QF-6	1.2	750	42	50	NO	1670	1.19	LEWIS
QF-9	1.2	700	15	11	NO	556	0.89	HAM-STD

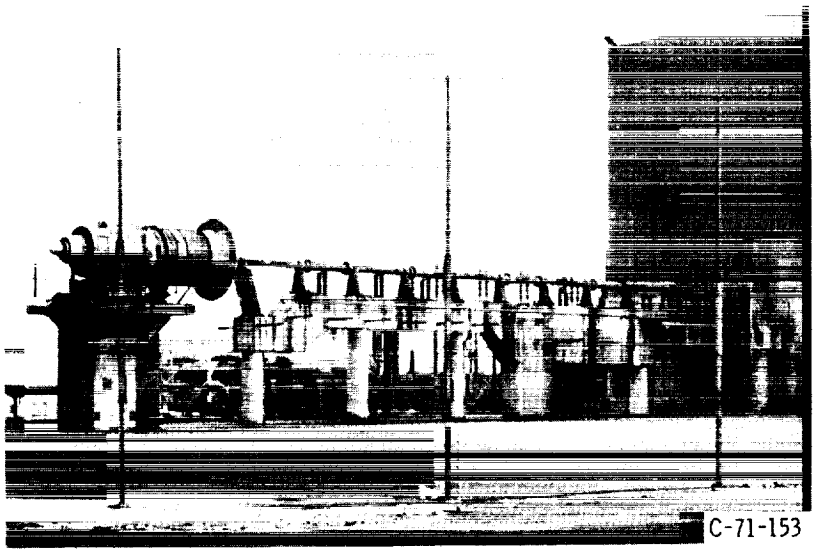

Figure 1. - Fan noise test facility with long shaft and front drive.

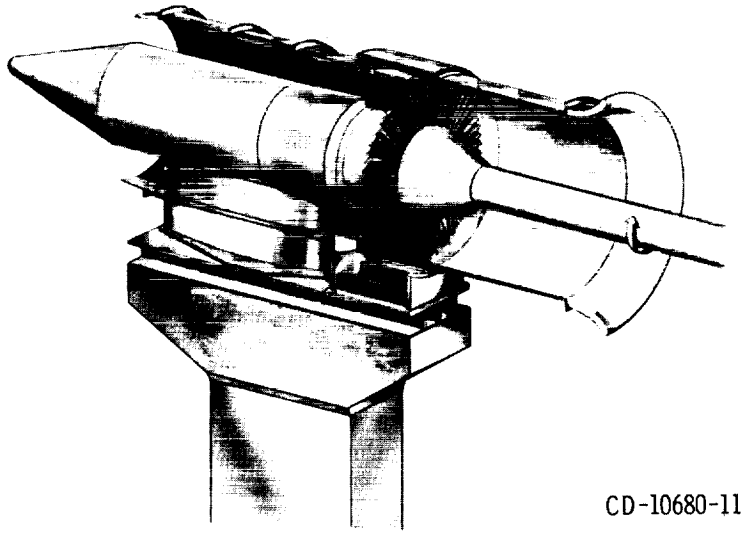

Figure 2. - Cutaway view of fan assembly.

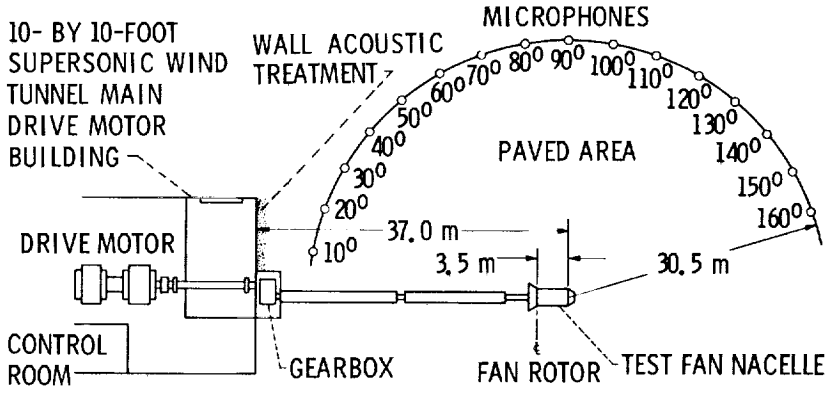

Figure 3. - Plan view of fan noise test facility.

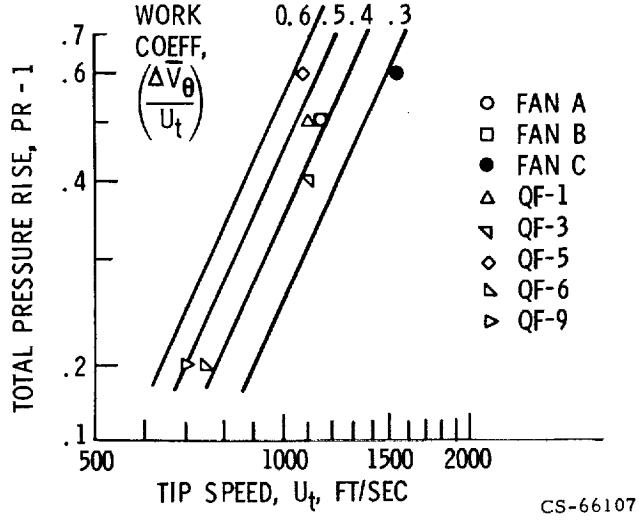

Figure 4. - Fan design variables.

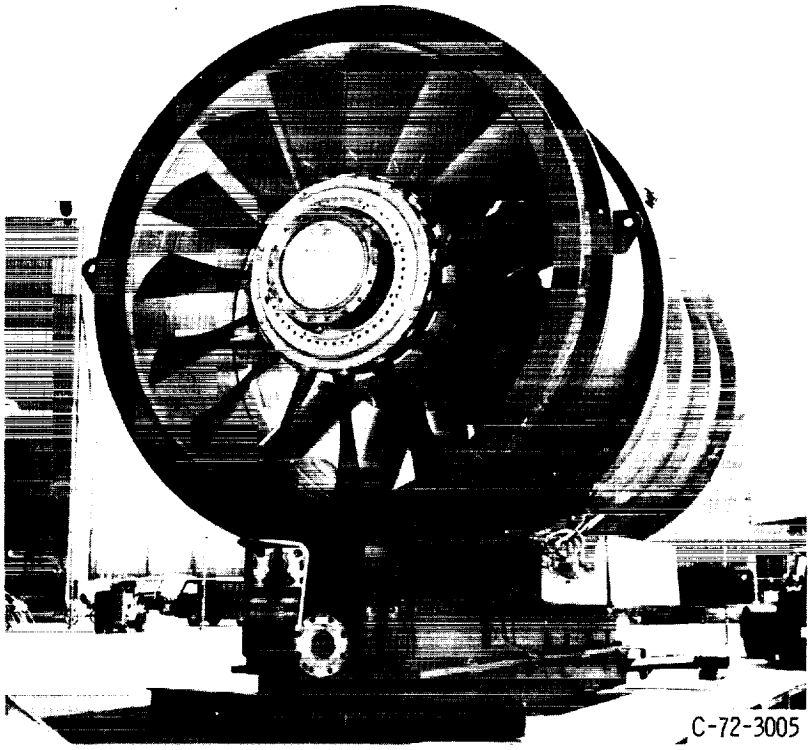

Figure 5. - Variable pitch fan QF-9.

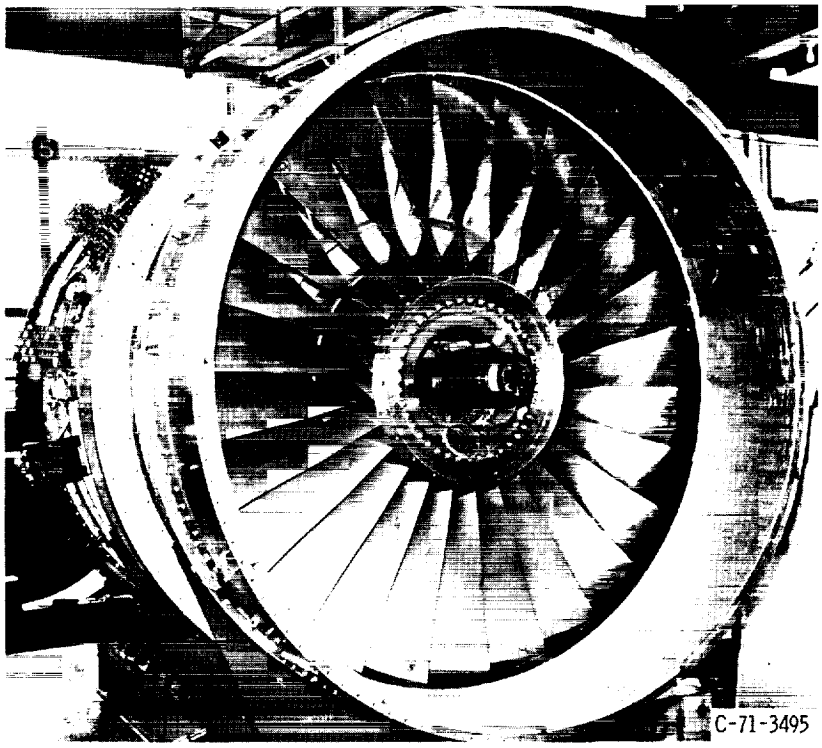

Figure 6. - Quiet engine - fan C.

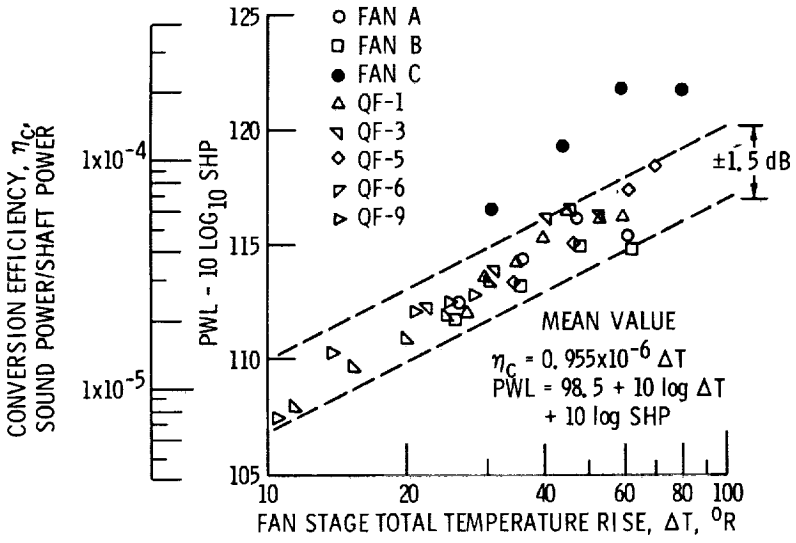

Figure 7. - Variation of conversion efficiency with fan stage total temperature rise, nominal operating line.

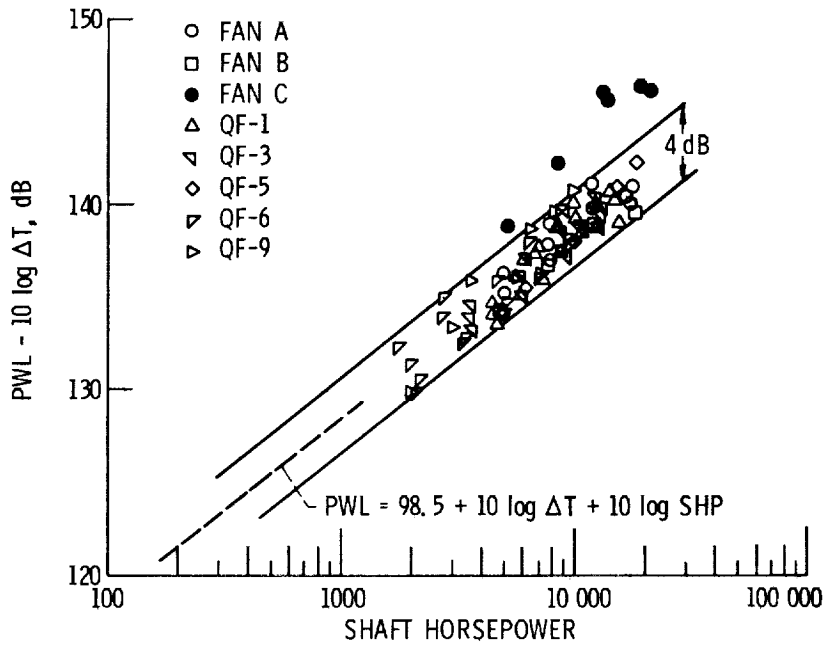

Figure 8. - Correlation of sound power with shaft horsepower and fan stage total temperature rise.

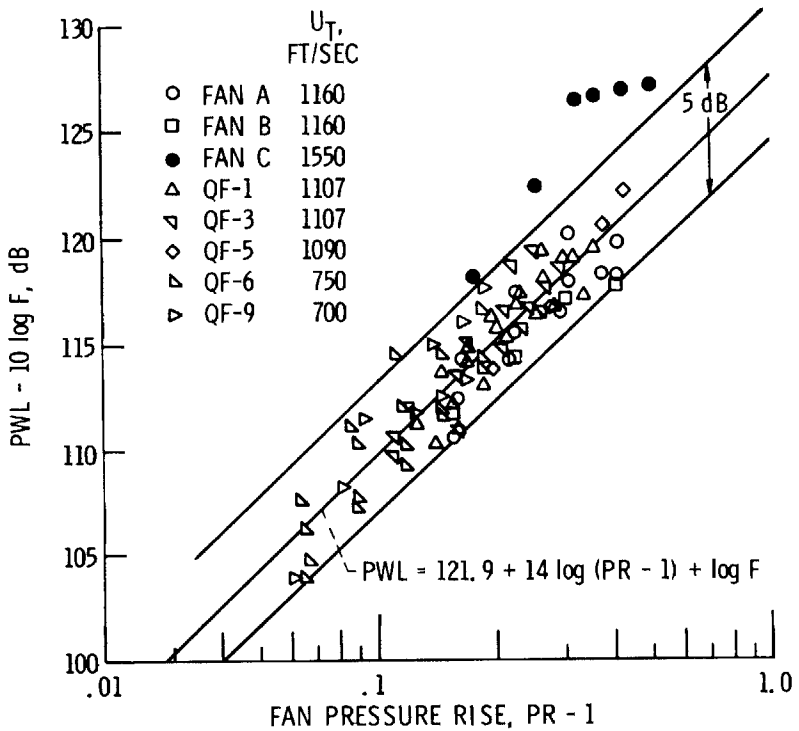

Figure 9. - Correlation of sound power from low tip speed fans.

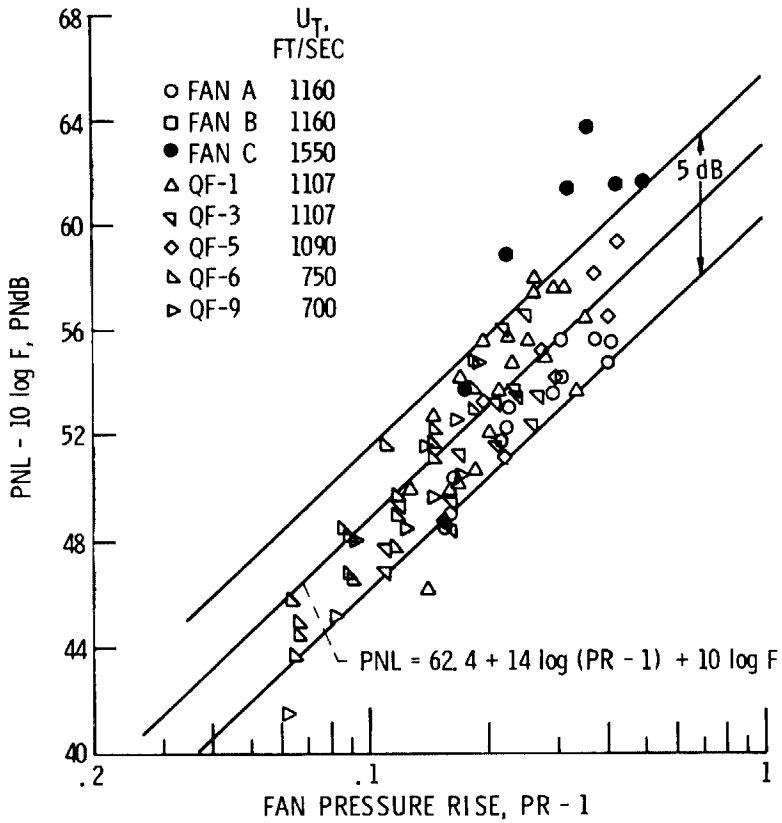

Figure 10. - Correlation of perceived noise from low tip speed fans. Maximum value, 1000-ft sideline.

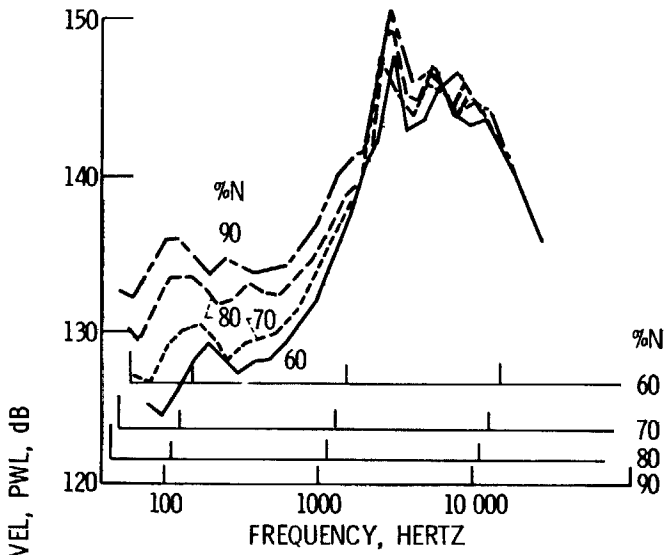

(a) Fan QF-3 at different tip speeds.

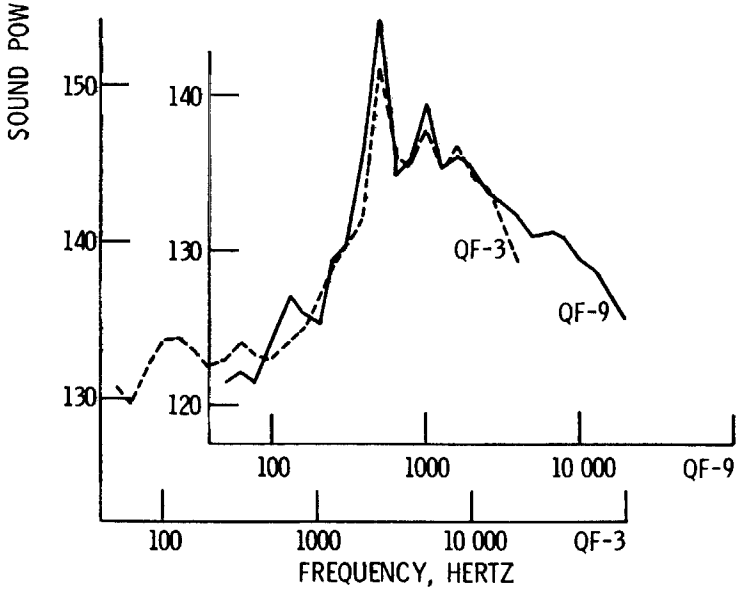

(b) Fans QF-3 and QF-9 at 85% and 86% design tip speed, respectively.

Figure 11. - Superposition of 1/3 octave sound power spectra.

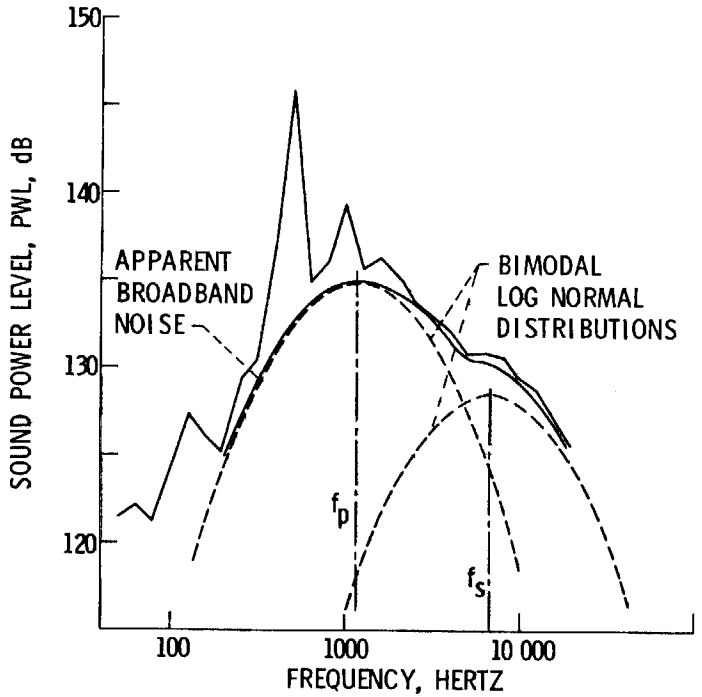

Figure 12. - Simulation of fan broadband noise spectra by bimodal log normal distribution function.

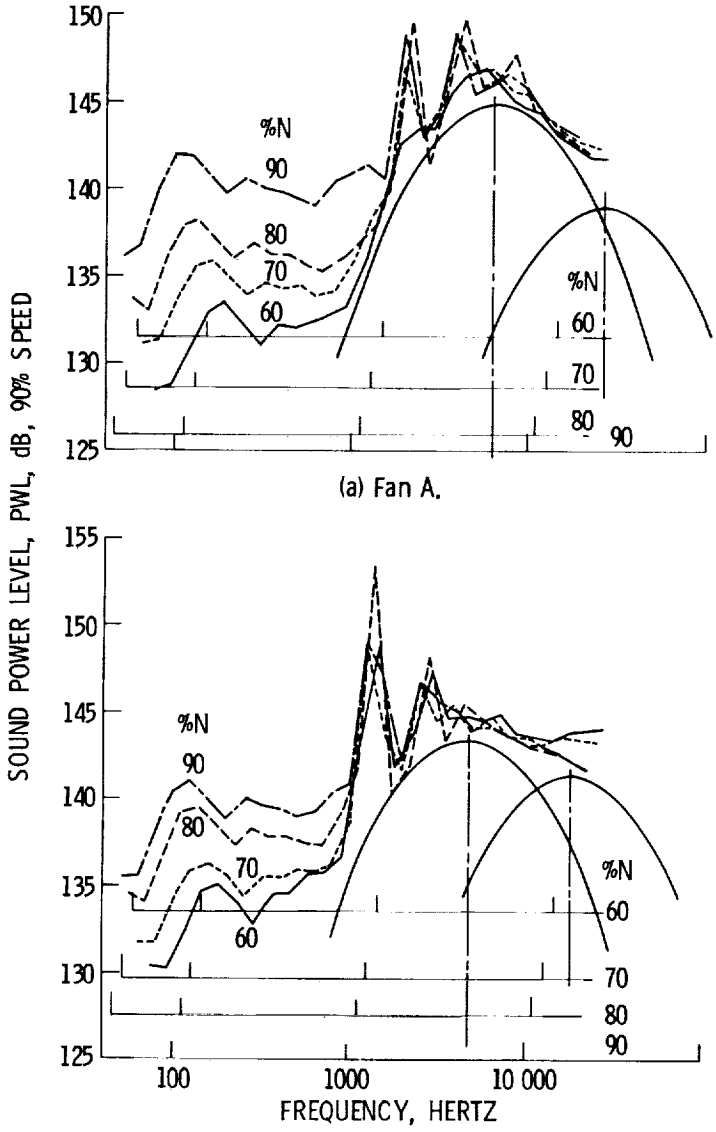

Figure 13. - Superimposed 1/3 octave total sound power spectra with fitted log normal broadband noise spectra.

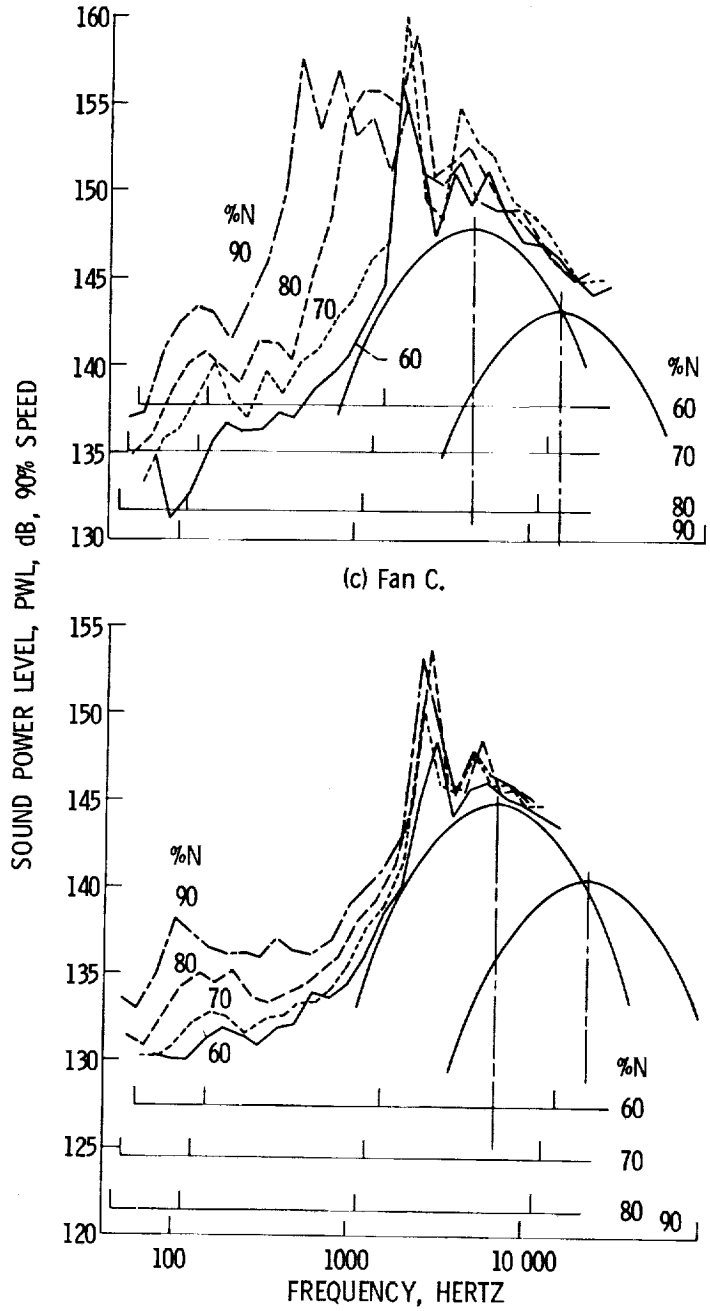

(c) Fan C.

(d) Fan QF-1.

Figure 13. - Continued.

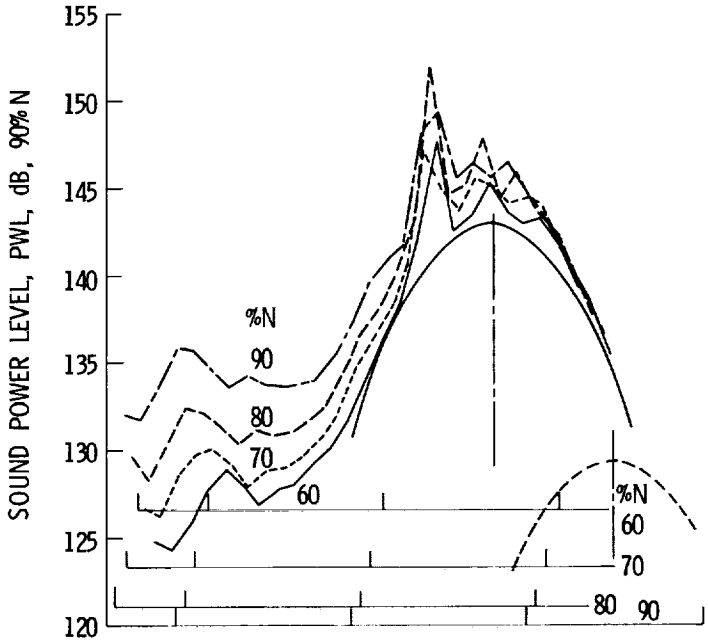

(e) Fan QF-3.

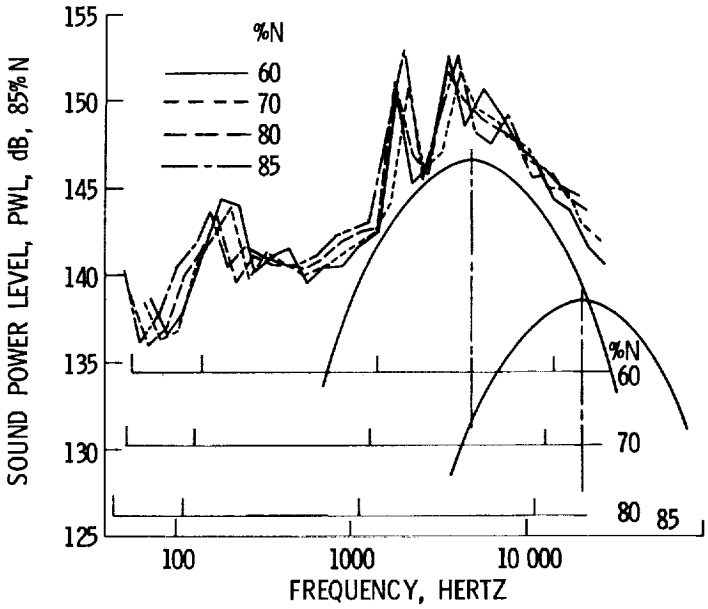

(f) Fan QF-5.

Figure 13. - Continued.

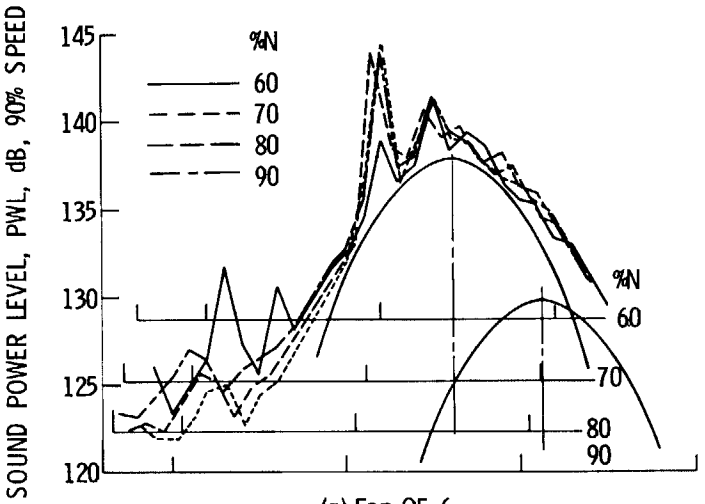

(g) Fan QF-6.

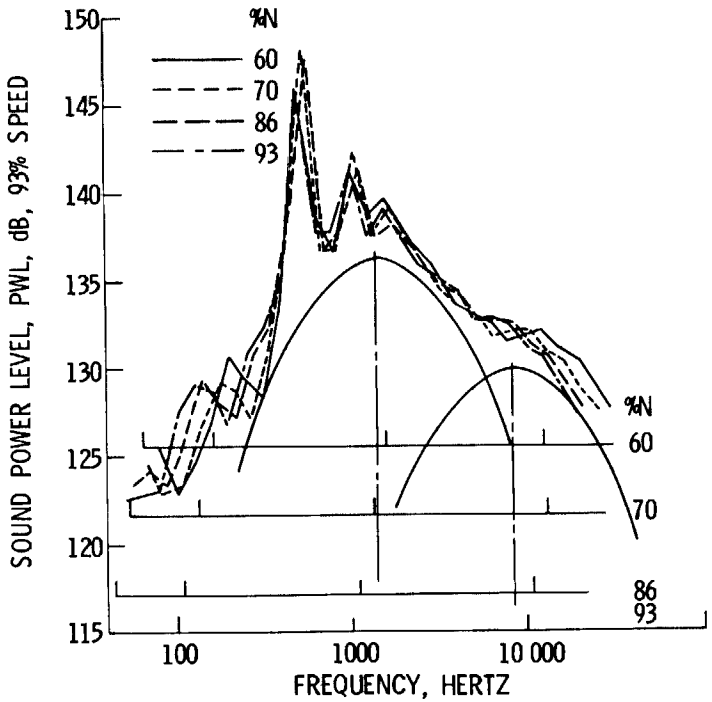

(h) Fan QF-9.

Figure 13. - Concluded.

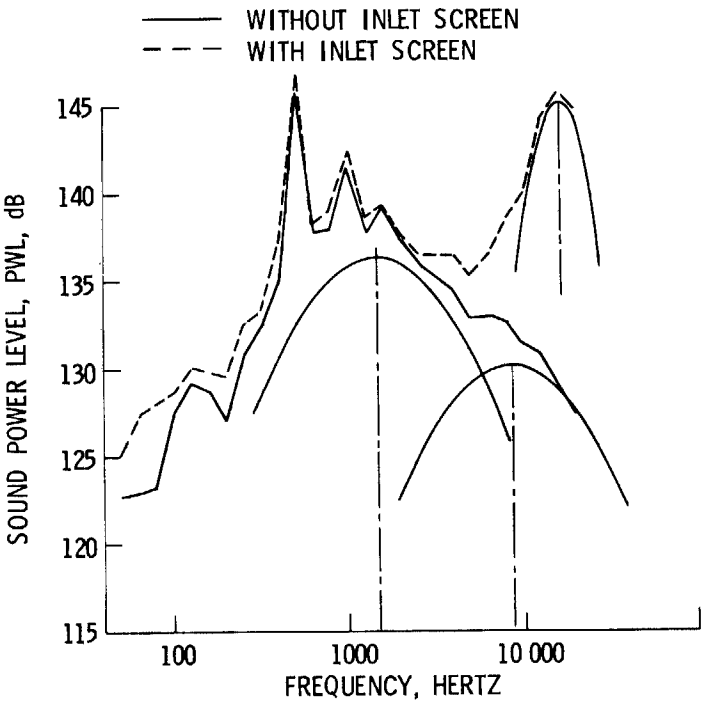

Figure 14. - Effect of inlet screen on sound power spectra. Fan QF-9; 93% speed.

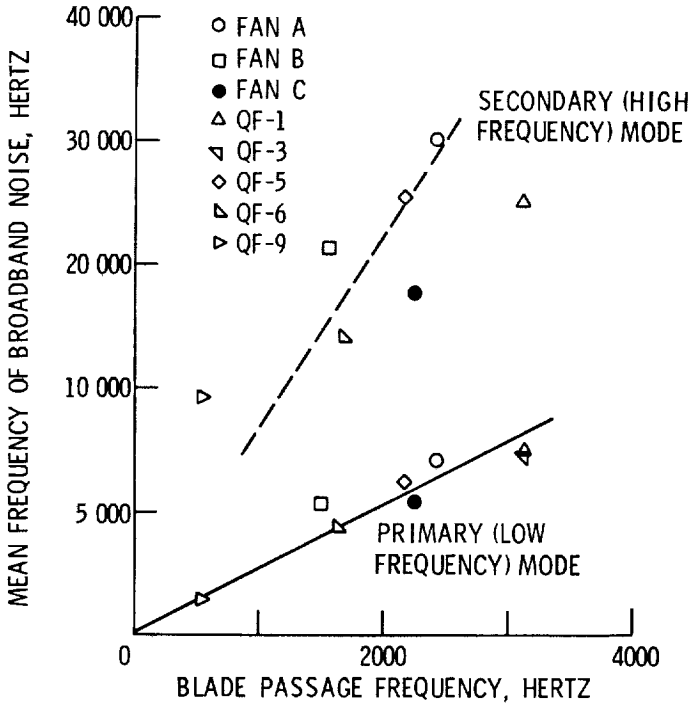

Figure 15. - Comparison of mean frequency of low and high frequency mode of broadband noise power with blade passage frequency.

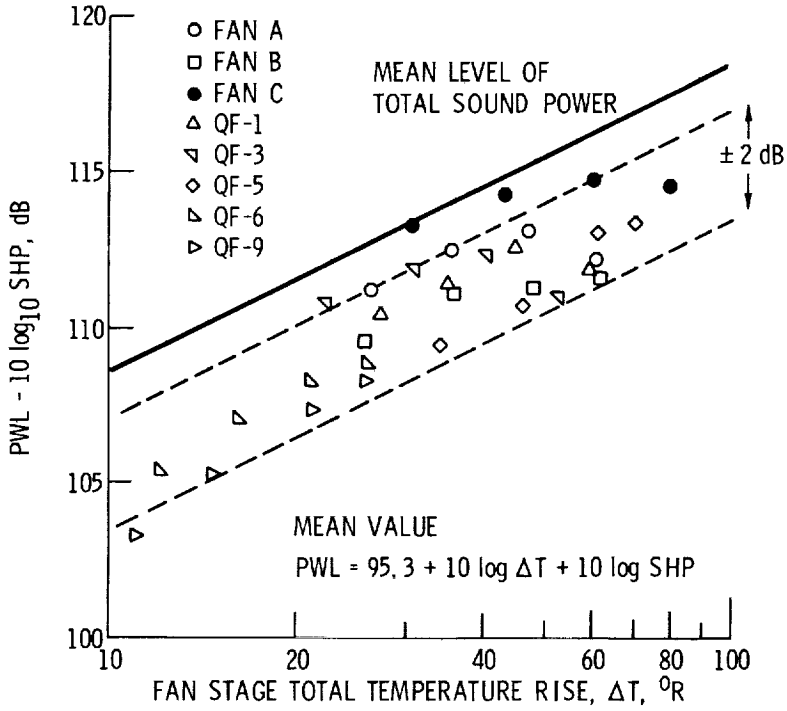

Figure 16. - Total broadband sound power level.

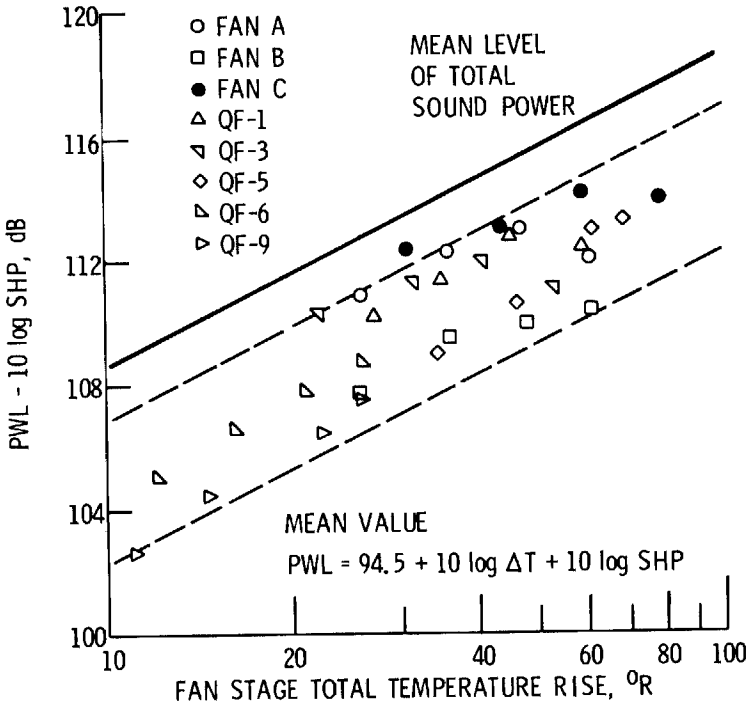

Figure 17. - Sound power content in low frequency mode of broadband noise.

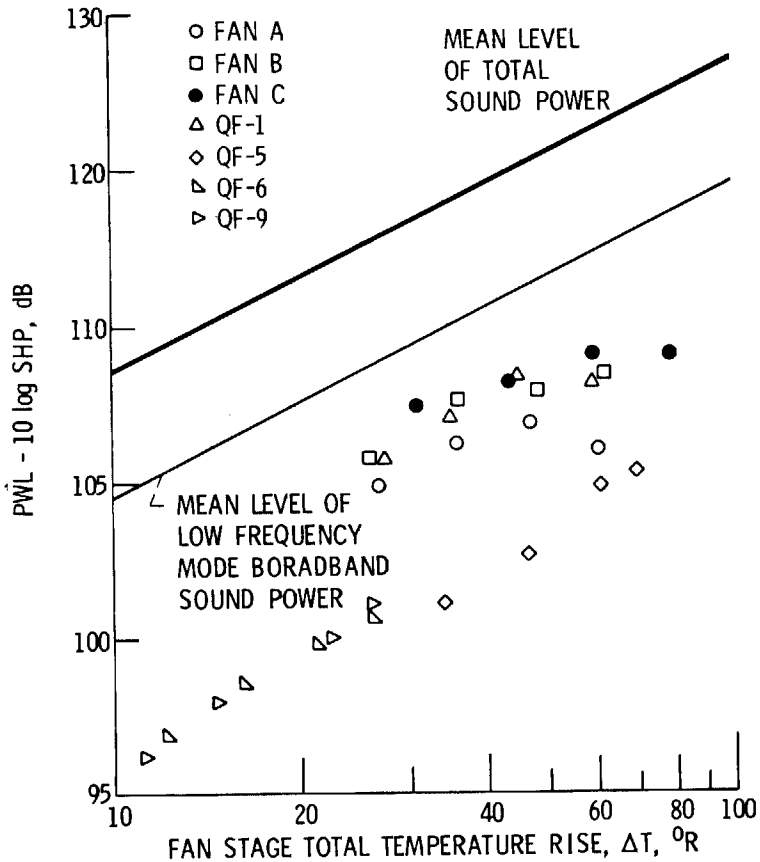

Figure 18. - Sound power content in high frequency mode of broadband noise.

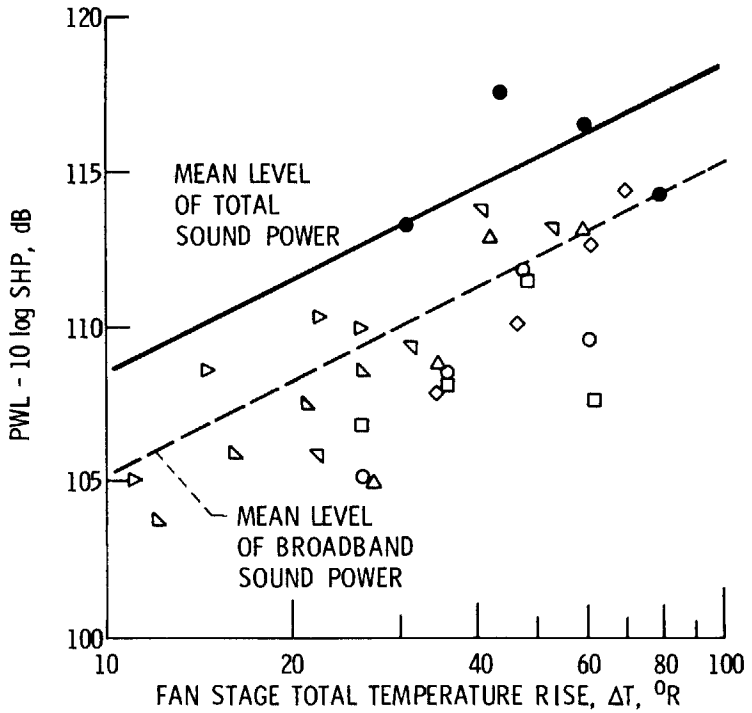

Figure 19. - Sound power level of blade passage tones as a function of total temperature rise.

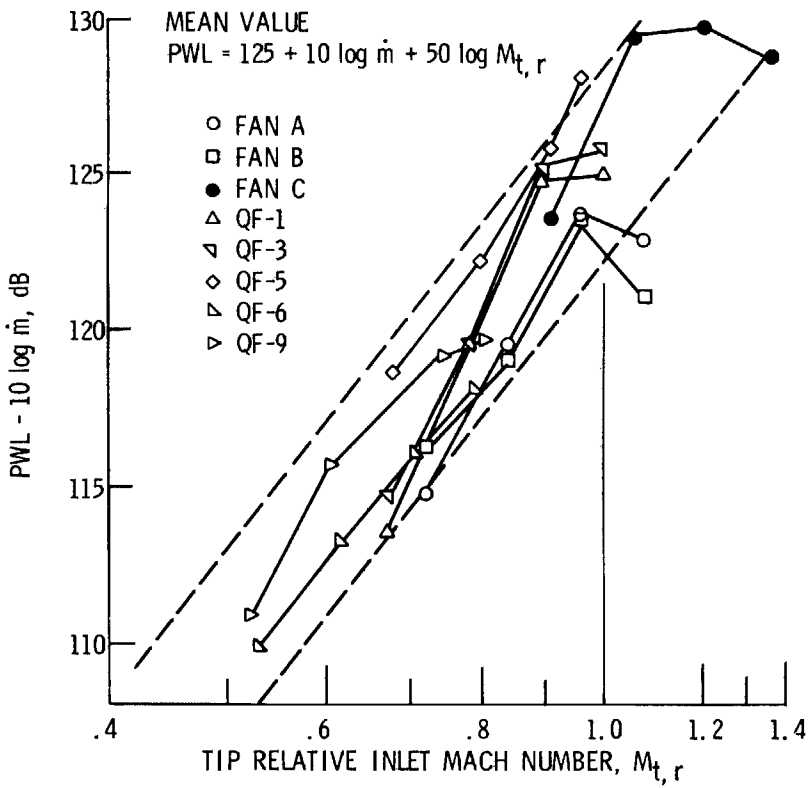

Figure 20. - Sound power level of blade passage tones as a function of tip relative inlet Mach number.